



HAL
open science

Pseudo-Darwinian evolution of physical flows in complex networks

Geoffroy C.B. Berthelot, Liubov Tupikina, Min-Yeong Kang, Bernard Sapoval, Denis S Grebenkov

► **To cite this version:**

Geoffroy C.B. Berthelot, Liubov Tupikina, Min-Yeong Kang, Bernard Sapoval, Denis S Grebenkov. Pseudo-Darwinian evolution of physical flows in complex networks. *Scientific Reports*, 2020, 10 (1), 10.1038/s41598-020-72379-8 . hal-02959924

HAL Id: hal-02959924

<https://insep.hal.science/hal-02959924v1>

Submitted on 7 Oct 2020

HAL is a multi-disciplinary open access archive for the deposit and dissemination of scientific research documents, whether they are published or not. The documents may come from teaching and research institutions in France or abroad, or from public or private research centers.

L'archive ouverte pluridisciplinaire **HAL**, est destinée au dépôt et à la diffusion de documents scientifiques de niveau recherche, publiés ou non, émanant des établissements d'enseignement et de recherche français ou étrangers, des laboratoires publics ou privés.



OPEN

Pseudo-Darwinian evolution of physical flows in complex networks

Geoffroy Berthelot^{1,2,3}, Liubov Tupikina^{4,5}, Min-Yeong Kang⁶, Bernard Sapoval⁶ & Denis S. Grebenkov⁶✉

The evolution of complex transport networks is investigated under three strategies of link removal: random, intentional attack and “Pseudo-Darwinian” strategy. At each evolution step and regarding the selected strategy, one removes either a randomly chosen link, or the link carrying the strongest flux, or the link with the weakest flux, respectively. We study how the network structure and the total flux between randomly chosen source and drain nodes evolve. We discover a universal power-law decrease of the total flux, followed by an abrupt transport collapse. The time of collapse is shown to be determined by the average number of links per node in the initial network, highlighting the importance of this network property for ensuring safe and robust transport against random failures, intentional attacks and maintenance cost optimizations.

Transport in complex systems can describe a variety of natural and human-engineered processes including biological^{1,2}, societal and technological ones^{3,4}. Common examples include blood vessel network and the lung airway tree⁵ that deliver blood and oxygen molecules, respectively; braided streams, consisting in a network of water channels, that occur in rivers and in glaciated landscapes when the discharge of water cannot transport its load or when sediment is deposited on the floor of the channel^{6,7}; transportation networks for passengers^{8–10}; social networks, in which the social and experience flow is progressively formed between individuals over time. These empirical networks are often scale-free and characterized by a degree distribution that follows a power law $P(k) \sim k^{-\gamma}$ with an exponent γ often in a range between 2 and 3 or a truncated power law^{11,12}. The morphological organization of transport in static scale-free networks was investigated from various perspectives^{13–16}. It is known that transport through scale-free networks and their functionality in general are vulnerable to the intentional attack to a few vertices with high degree, but remain very robust to random failures^{17,18}. While the percolation by deleting *nodes* has been extensively studied^{15,19,20}, the effect of progressive *link* removal on transport in scale-free networks is not well understood. In this paper we aim at investigating how the temporal evolution of local connectivities can lead to emergence of ordered structures in scale-free networks under different strategies of link removal. While we will focus on physical transport systems, where a flux is an electric current or the quantity of transferred materials or molecules over time, the obtained results are of much broader scope and reveal the fundamental principles of structural evolution of general transport networks.

Methods

We construct a random scale-free network on an $n \times n$ square lattice. Its links are generated by using the uncorrelated configuration model²¹ with a given degree exponent γ . We consider the resistance $r_{i,j}$ of each link as a function of the Euclidean distance $d_{i,j}$ between the nodes i and j : $r_{i,j} = d_{i,j}^\beta$, with an exponent β . In an electric or hydraulic circuit, the resistance of a wire or a tube is proportional to its length, and $\beta = 1$. In turn, most former studies on transport in resistor networks supposed constant link resistance, i.e., $\beta = 0$. In each random realization of the resistor network with prescribed exponents γ and β , we select randomly a source and a drain nodes, at which the potential is fixed to be 1 and 0, respectively. We ensure the distance (in terms of the number of nodes)

¹Centre de Mathématiques Appliquées, CNRS – Ecole Polytechnique, IP Paris, 91128 Palaiseau, France. ²Research Laboratory for Interdisciplinary Studies (RELAIS), 75012 Paris, France. ³Institut National du Sport, de l'Expertise et de la Performance (INSEP), 75012 Paris, France. ⁴Center for Research and Interdisciplinarity (CRI), Université de Paris – INSERM (U1284), 75004 Paris, France. ⁵Bell Labs Nokia, Paris, France. ⁶Laboratoire de Physique de la Matière Condensée (UMR 7643), CNRS – Ecole Polytechnique, IP Paris, 91128 Palaiseau, France. ✉email: denis.grebenkov@polytechnique.edu

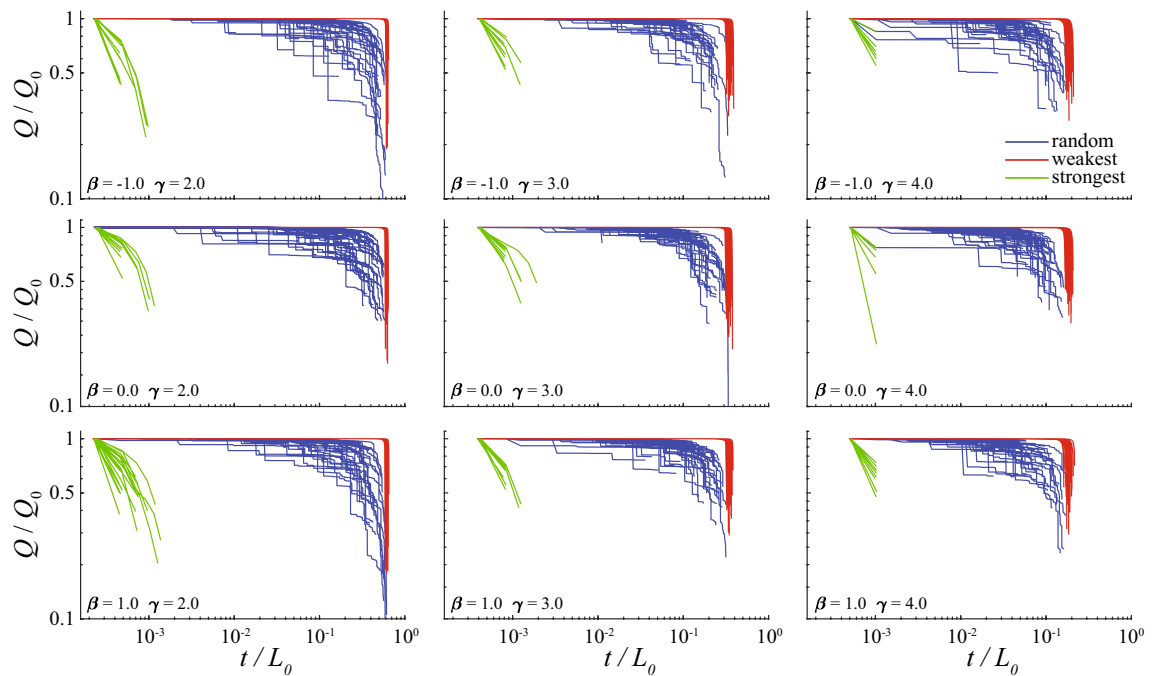


Figure 1. Evolution of the total flux Q (rescaled by Q_0) for a scale-free network with $N_0 = 40 \times 40$ nodes for nine combinations of parameters γ and β : $\gamma = \{2, 3, 4\}$ (left, middle and right columns) and $\beta = \{-1, 0, 1\}$ (top, middle and bottom rows). In each plot, 60 curves correspond to 60 random realizations of the initial network.

between the source and drain is ≥ 4 . The system of linear Kirchhoff's equations²² for the potential on other nodes is solved numerically using a custom routine in Matlab. Then the distributions of nodes potentials and currents in links are obtained. Such a point-to-point transport was shown to be self-organized into two tree-like structures, one emerging from the source and the other converging to the drain¹⁶. These trees merge into a large cluster of the remaining nodes that is found to be quasi-equipotential and thus presents almost no resistance to transport.

We consider three dynamics of network evolution, in which links are progressively removed according to one of the following strategies: at each step, one removes (i) randomly chosen link, (ii) the link with the strongest flux, and (iii) the link with the weakest flux. These three evolution strategies are meant to model respectively (i) progressive failures in a system in random (unrelated) places (e.g., due to material aging); (ii) intentional attacks on the network by removing the most relevant links; and (iii) a kind of progressive optimization of the system by removing least used elements. While the first two evolution strategies have been earlier studied (but mainly for nodes removal)²³, we are not aware of former works on the latter network evolution that we call “Pseudo-Darwinian strategy” of network percolation. Such a strategy is often employed in nature, e.g., as the mechanism of capillary network remodeling during morphogenesis²⁴.

At each evolution step, we first solve the system of Kirchhoff's equations to calculate fluxes in all links, and then we remove a link according to the selected strategy. After link removal, we also remove “dead-ends” (i.e., nodes that have a single link), thus imposing that any existing node after an evolutionary step has at least two links. We keep track of the *total flux* Q , i.e., the flux that enters into the network from the source node. As we investigate the evolution of the network after successive link removals, it is natural to associate the number of evolution steps with “time” t , with 0 being the initial time, before the evolution takes place. We denote Q_0 , L_0 and $N_0 = n^2$ as the total flux, the number of links, and the number of nodes of the initial network, respectively. The evolution ends when at least one of the following conditions is met: (i) no path exists between the source and the drain (i.e. the source and drain are disconnected), (ii) the source or the drain is removed from the network, (iii) a portion of the network—a subgraph containing more than one node—is disconnected from the rest of the network containing the source and drain. We call this moment as “time of collapse” t_c : as one of the previous conditions is met, transport is no longer maintained through the whole network.

Results

We first explore a scale-free resistor network with $N_0 = 40 \times 40$ nodes and parameters $\gamma \in \{2, 3, 4\}$ and $\beta \in \{-1, 0, 1\}$. Figure 1 shows how the total flux Q , rescaled by its initial value Q_0 , evolves with time t for different networks (γ , β) and strategies. Expectedly, the progressive removal of the strongest links leads to a very rapid transportation collapse, whereas this decline is the slowest for the pseudo-Darwinian strategy. To better understand the effect of this strategy, we also calculate the derivative of the total flux Q with respect to time (Fig. 2). Two regimes are observed: a slow, power law decay, followed by an abrupt decay. In the first regime, we find the universal scaling exponent 2 of the derivative of the total flux for all γ and β values, implying

$$Q(t)/Q_0 \simeq 1 - C(t/t_c)^3 \quad (t \ll t_c), \quad (1)$$

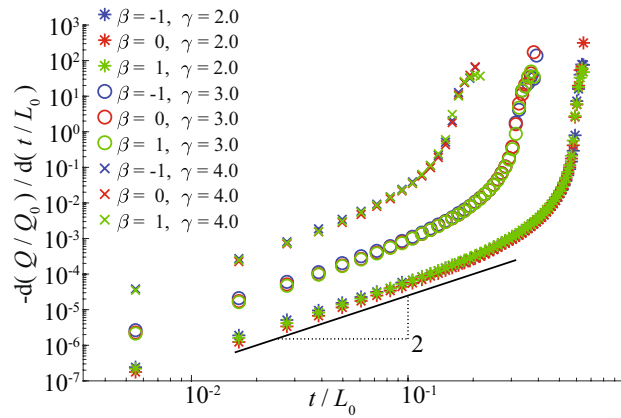


Figure 2. Time derivative of the total flux for a scale-free network with $N_0 = 40 \times 40$ nodes and different values of γ and β for the pseudo-Darwinian strategy only. The slope is identical for all values of γ and β , suggesting a universal phenomenon. The derivative here is calculated as an average from 60 realizations.

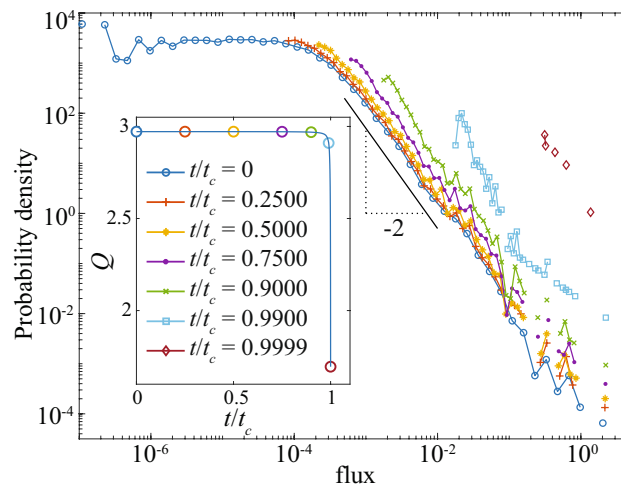


Figure 3. The flux probability density at selected moments of t/t_c , for a network with $N_0 = 100 \times 100$ nodes, $\gamma = 2.5$, $\beta = 1$, and $L_0 = 21,040$ initial links. Corresponding total fluxes are shown in the inset.

where C is a nonuniversal constant. The distribution of fluxes in links along the evolution process (Fig. 3) shows that the removal of the weakest link at each evolution step does not affect the distribution of large fluxes for the most period of evolution. For this period, the total flux remains almost the same. Figure 4 helps to understand this robustness: the removal occurs mostly in the links in the quasi-equipotential cluster where connections are abundant while the links with large currents are kept.

The time of collapse t_c is related to the degree exponent γ in all strategies: networks with lower γ values produce higher t_c (Fig. 1). This highlights the role of connectivity in resisting against random or targeted attacks. This effect is illustrated for the pseudo-Darwinian evolution by plotting the time of collapse rescaled by L_0 , t_c/L_0 , versus the initial number of links L_0 for various network sizes (Fig. 5(left)). Further rescaling the horizontal axis L_0 by the initial number of nodes, N_0 , results in a collapse of all curves into a single master curve that determines t_c/L_0 as a function of the initial average degree, L_0/N_0 , independently of the network structure (γ, β) and size N_0 (Fig. 5(right)). Thus we conclude that higher average degree in an initial network helps in delaying the time t_c of transport collapse.

Discussion

In our setup, the total flux describes a network functionality and its ability to transport or distribute a current. Thus, the sudden collapse observed in all three strategies means that the network eventually fails to transport. The onset of this collapse is affected by the evolution strategy, in particular, the pseudo-Darwinian strategy leads to a nearly “optimized” network, i.e. a structure that carries most of the flux with minimal number of useless links (i.e. links that carry a negligible part of the flux). This can also be seen as an “economical” structure, where the transport function is kept with the least size of components and, hence, minimized maintenance cost²⁵.

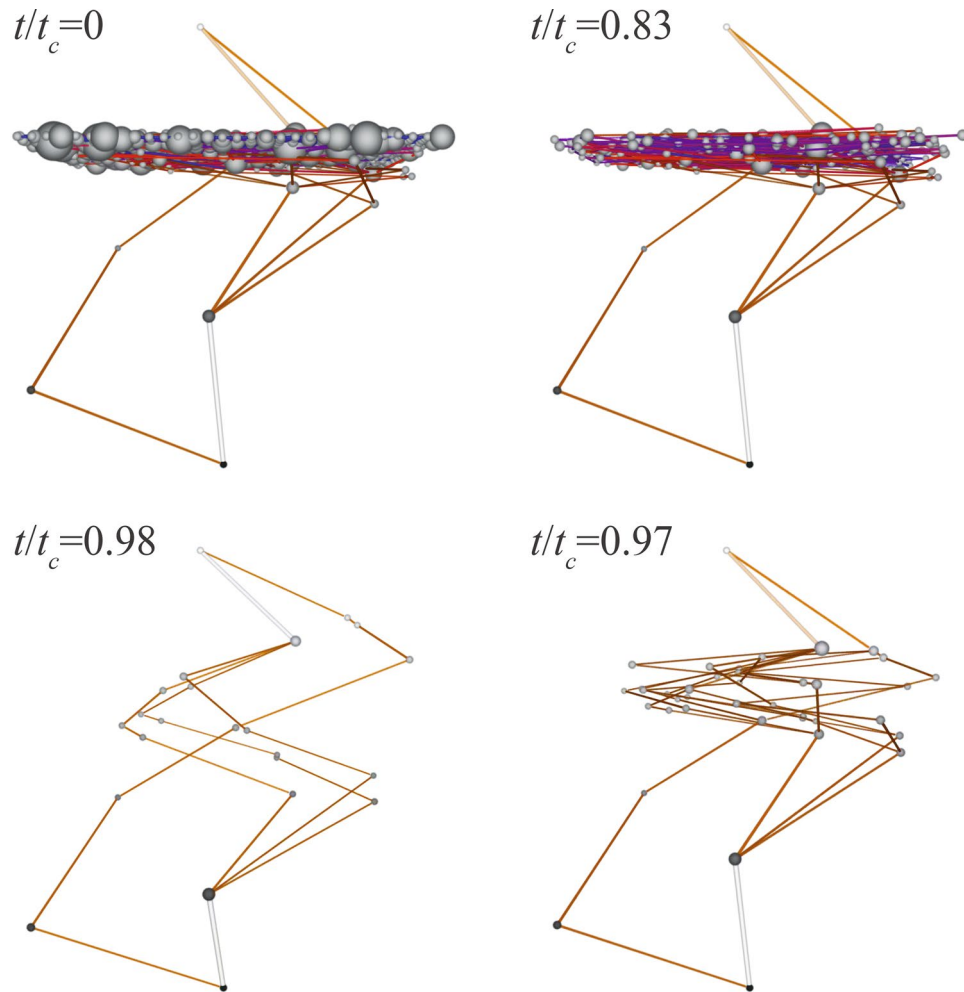


Figure 4. Visualization of evolution of a scale-free network (with $N_0 = 30 \times 30$ nodes, $\gamma = 2.5$ and $\beta = 1$; A video is available online). Each node of the network is shown by a ball whose radius is proportional to the square root of its connectivity. The planar coordinates of the balls are the positions of the corresponding nodes on the square lattice, whereas the height Z represents the potential at the node by a linear relation $Z = V$. Each link brightness is proportional to the magnitude of its current (in addition, blue colors are used for very small currents). The quasi-equipotential cluster is qualitatively identified as a large ensemble of nodes almost at the same potential. Four panels represent the network at four moments, t/t_c , during evolution (clock-wise direction): 0 (initial state), 0.83, 0.97, and 0.98. Along the evolution process, the weakest links are removed successively. Note that links in the cluster are removed during the majority of evolution period.

However, going to an optimal system makes it fragile and dangerous because a small disturbance can lead to a sudden collapse. Therefore, for robustness of the network, a safety margin from the critical point t_c should be considered, as known for human bronchial systems⁵.

When reaching t_c , the “optimized” structure becomes a chain connecting pre-selected source and drain nodes. While this structure is formally optimal, it is impractical for applications due to its “optimality” for the particular choice of the source and the drain. A much more challenging and practically relevant question would be the construction of the optimal structure for all (or for most) pairs of source and drain nodes. This problem will be investigated in a subsequent work.

This paper focused on the evolution of both transport and structural properties of scale-free networks under progressive link removal. Such transport-driven dynamics further extend common models of network evolutions^{26–28}. In particular, our analysis helps to investigate the precursors of the transitions for links percolation applied to resistor networks²⁹ or epidemic spreading³⁰. More generally, this study can serve as a basis for illustrating generic evolution dynamics of complex networks governed by its transport properties. Different works already made the analogy between Kirchhoff’s laws and the conservation of mass equation, with applications to vehicular flow³¹, fractures in materials³², neuronal circuitry in the brain³³. For instance, a direct analogy with random walks on graphs opens exciting perspectives for understanding diffusive transport and first-passage processes on evolving networks^{34,35}. Our approach is also expected to stimulate further studies of link-based percolation in other networks such as in protein networks, where links can be lost with time (corresponding to the loss of some proteins’ functionalities), while proteins, the nodes of a network, remain present³⁶.

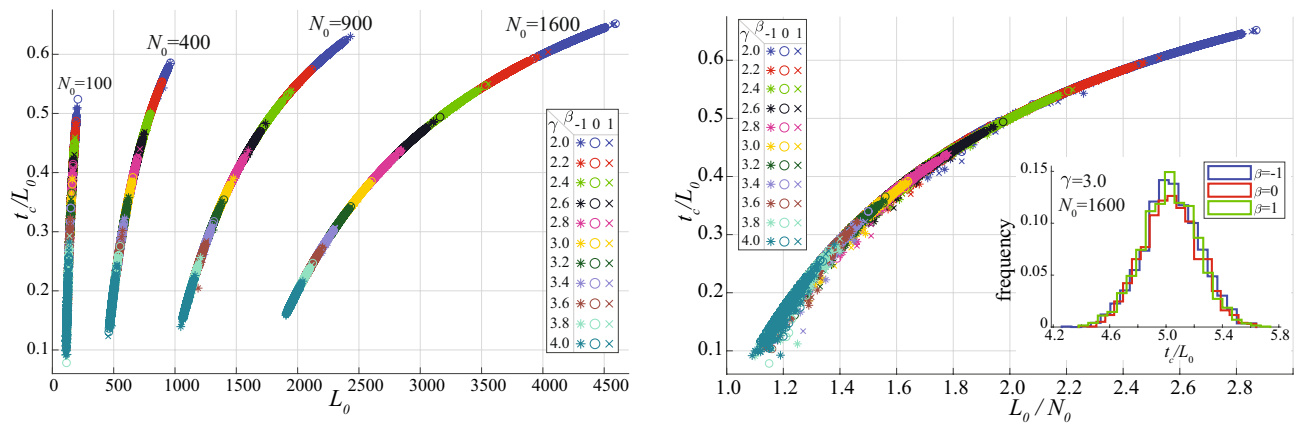


Figure 5. Rescaled time of collapse t_c/L_0 versus the initial number of links L_0 (**left**) or versus the average initial number of links per node L_0/N_0 (**right**) for 4 different network sizes ($N_0 = 100$, $N_0 = 400$, $N_0 = 900$, $N_0 = 1600$), 11 values of γ (evenly spaced from 2 to 4) and 3 values of β ($\beta = \{-1, 0, 1\}$). Each colored marker represents the time of collapse obtained from 200 realizations for each triplet of γ (specified by color), β (specified by marker) and network size N_0 . The parameter β has no significant effect on t_c , as confirmed in the inset, where three colored lines show the empirical distributions of t_c for three different values of β (obtained from 2,000 simulations).

Data availability

Data sharing not applicable to this article as no datasets were generated or analysed during the current study.

Received: 29 February 2020; Accepted: 28 July 2020

Published online: 23 September 2020

References

1. Grebenkov, D. S., Filoche, M., Sapoval, B. & Felici, M. Diffusion-reaction in branched structures: theory and application to the lung acinus. *Phys. Rev. Lett.* **94**, 050602 (2005).
2. Serov, A. S., Salafia, C., Grebenkov, D. S. & Filoche, M. The role of morphology in mathematical models of placental gas exchange. *J. Appl. Physiol.* **120**, 17–28 (2016).
3. Lambiotte, R. *et al.* Flow graphs: interweaving dynamics and structure. *Phys. Rev. E* **84**, 017102 (2011).
4. Newman, M. E. J. & Girvan, M. Finding and evaluating community structure in networks. *Phys. Rev. E* **69**, 026113 (2004).
5. Mauroy, B., Filoche, M., Weibel, E. R. & Sapoval, B. An optimal bronchial tree may be dangerous. *Nature* **427**, 633–636 (2004).
6. Connor-Streich, G., Henshaw, A. J., Brasington, J., Bertoldi, W. & Harvey, G. L. Let's get connected: a new graph theory-based approach and toolbox for understanding braided river morphodynamics. *WIREs Water* **5**, e1296 (2018).
7. Rinaldo, A., Rigon, R., Banavar, J. R., Maritan, A. & Rodriguez-Iturbe, I. Evolution and selection of river networks: statics, dynamics, and complexity. *Proc. Nat. Acad. Sci. USA* **111**, 2417–2424 (2014).
8. Mattsson, L. G. & Jenelius, E. Vulnerability and resilience of transport systems—a discussion of recent research. *Transp. Res. A* **81**, 16–34 (2015).
9. von Ferber, C., Berche, B., Holovatch, T. & Holovatch, Y. A tale of two cities. *J. Transp. Secur.* **5**, 199–216 (2012).
10. Zhang, L., Lu, J., Fu, B. B. & Li, S. B. A review and prospect for the complexity and resilience of urban public transit network based on complex network theory. *Complexity* **2018**, 2156309 (2018).
11. Barabási, A. L. & Albert, R. Emergence of scaling in random networks. *Science* **286**, 509–512 (1999).
12. Wu, Z. *et al.* Current flow in random resistor networks: the role of percolation in weak and strong disorder. *Phys. Rev. E* **71**, 045101(R) (2005).
13. López, E., Buldyrev, S. V., Havlin, S. & Stanley, H. E. Anomalous transport in scale-free networks. *Phys. Rev. Lett.* **94**, 248701 (2005).
14. López, E., Parshani, R., Cohen, R., Carmi, S. & Havlin, S. Limited path percolation in complex networks. *Phys. Rev. Lett.* **99**, 188701 (2007).
15. Nicolaides, C., Cueto-Felgueroso, L. & Juanes, R. Anomalous physical transport in complex networks. *Phys. Rev. E* **82**, 055101(R) (2010).
16. Kang, M. Y. *et al.* Morphological organization of point-to-point transport in complex networks. *Sci. Rep.* **9**, 8322 (2019).
17. Goh, K. I., Kahng, B. & Kim, D. Packet transport and load distribution in scale-free network models. *Physica A* **318**, 72–79 (2003).
18. Valente, A. X. C. N., Sarkar, A. & Stone, H. A. Two-peak and three-peak optimal complex networks. *Phys. Rev. Lett.* **92**, 118702 (2004).
19. Havlin, S. & Ben-Avraham, D. Diffusion in disordered media. *Adv. Phys.* **51**, 187–292 (2002).
20. Gouyet, J.-F., Rosso, M. & Sapoval, B. Fractal structure of diffusion and invasion fronts in three-dimensional lattices through the gradient percolation approach. *Phys. Rev. B* **37**, 1832–1838 (1988).
21. Pastor-Satorras, R. & Vespignani, A. *Evolution and Structure of the Internet: A Statistical Physics Approach* (Cambridge University Press, Cambridge, 2007).
22. Redner, S. *A Guide to First-Passage Processes* (Cambridge University Press, Cambridge, 2001).
23. Gallos, L. K., Cohen, R., Argyrakis, P., Bunde, A. & Havlin, S. Stability and topology of scale-free networks under attack and defense strategies. *Phys. Rev. Lett.* **94**, 188701 (2005).
24. Le Noble, F. *et al.* Flow regulates arterial-venous differentiation in the chick embryo yolk sac. *Development* **131**, 361–375 (2004).
25. Murray, C. D. The physiological principle of minimum work: I. The vascular system and the cost of blood volume. *Proc. Nat. Acad. Sci. USA* **12**, 207–214 (1926).
26. Dorogovtsev, S. N. & Mendes, J. F. F. Evolution of networks. *Adv. Phys.* **51**, 1079–1187 (2002).

27. Dorogovtsev, S. N., Goltsev, A. V. & Mendes, J. F. F. Critical phenomena in complex networks. *Rev. Mod. Phys.* **80**, 1275–1335 (2008).
28. Garlaschelli, D., Capocci, A. & Caldarelli, G. Self-organized network evolution coupled to extremal dynamics. *Nat. Phys.* **3**, 813–817 (2007).
29. Rodriguez, V., Eguiluz, V., Hernandez-Garcia, E. & Ramasco, J. J. Percolation-based precursors of transitions in extended systems. *Sci. Rep.* **6**, 29552 (2016).
30. Sander, L. M., Warren, C. P. & Sokolov, I. M. Epidemics, disorder, and percolation. *Physica A* **325**, 1–8 (2003).
31. Guarnaccia, C. Analysis of traffic noise in a road intersection configuration. *WSEAS Trans. Syst.* **8**, 865–874 (2010).
32. Batrouni, G. G. & Hansen, A. Fracture in three-dimensional fuse networks. *Phys. Rev. Lett.* **80**, 325–328 (1998).
33. Destexhe, A. & Bedard, C. Do neurons generate monopolar current sources?. *J. Neurophysiol.* **108**, 953–955 (2012).
34. Condamin, S., Bénichou, O., Tejedor, V., Voituriez, R. & Klafter, J. First-passage time in complex scale-invariant media. *Nature* **450**, 77–80 (2007).
35. Tupikina, L. & Grebenkov, D. S. Structural and temporal heterogeneities on networks. *Appl. Net. Sci.* **4**, 16 (2019).
36. Kovács, I. A. *et al.* Network-based prediction of protein interactions. *Nat. Commun.* **10**, 1240 (2019).

Acknowledgements

We thank Jean-François Colonna for the creation of the video showing the evolution of the network (Fig. 4). L. T. acknowledges a partial financial support via the CRI Research Fellowship thanks to the Bettencourt Schueller Foundation long term partnership. D. S. G. acknowledges a partial financial support from the Alexander von Humboldt Foundation through a Bessel Research Award.

Author contributions

B.S. and D.S.G. conceived the research project, M.Y.K., G.B. and L.T. performed numerical computations, G.B., M.Y.K., and D.S.G. prepared figures, D.S.G., B.S., L.T., M.Y.K. and G.B. analyzed the results and wrote the manuscript. All authors reviewed the manuscript.

Competing interests

The authors declare no competing interests.

Additional information

Supplementary information is available for this paper at <https://doi.org/10.1038/s41598-020-72379-8>.

Correspondence and requests for materials should be addressed to D.S.G.

Reprints and permissions information is available at www.nature.com/reprints.

Publisher's note Springer Nature remains neutral with regard to jurisdictional claims in published maps and institutional affiliations.



Open Access This article is licensed under a Creative Commons Attribution 4.0 International License, which permits use, sharing, adaptation, distribution and reproduction in any medium or format, as long as you give appropriate credit to the original author(s) and the source, provide a link to the Creative Commons licence, and indicate if changes were made. The images or other third party material in this article are included in the article's Creative Commons licence, unless indicated otherwise in a credit line to the material. If material is not included in the article's Creative Commons licence and your intended use is not permitted by statutory regulation or exceeds the permitted use, you will need to obtain permission directly from the copyright holder. To view a copy of this licence, visit <http://creativecommons.org/licenses/by/4.0/>.

© The Author(s) 2020